Environmental Pollution 405 (2026) 128517

Contents lists available at ScienceDirect

Environmental Pollution

journal homepage: www.elsevier.com/locate/envpol

Rainfall-driven, high-resolution assessment of water acidification in a planned reservoir within an unreclaimed historical mining basin

Jonatan Romero-Matos *, Laura Sánchez-López, Rafael León, Francisco Macías, Carlos R. Cánovas, Manuel Olías, José Miguel Nieto

Department of Earth Sciences & Research Center on Natural Resources, Health and the Environment, University of Huelva, Campus "El Carmen", Huelva, 21071, Spain

ARTICLE INFO

Keywords:
High-resolution sampling
Iberian pyrite belt (IPB)
Alcolea reservoir
Acid mine drainage (AMD)
Flood events

ABSTRACT

Acid mine drainage (AMD) from historical mining in the Iberian Pyrite Belt severely degrades water quality in southwest Spain. The planned Alcolea Reservoir, intended to supply water from the Odiel River basin in response to growing demands, is widely recognized as being critically constrained by AMD, as existing studies indicate that, without upstream remediation, its impoundment would lead to inevitable deterioration and acidification of water quality. In this sense, a high-resolution sampling campaign was conducted over a hydrological year in the Odiel and Oraque rivers to quantify pollutant fluxes entering the reservoir and to assess the potential risk of water acidification. Despite dilution- and neutralization-driven fluctuations, the inflows showed mostly persistent acidic conditions and high metal concentrations during the monitored year. Floods were the main driver of pollutant transport, with annual net acidity and sulfate loads about 31247 tons eq. $CaCO_3$ and 73598 tons, respectively. During the autumn floods, the highest amounts of acidity and metals were released due to flush-out processes (i.e., redissolution of evaporitic sulfate salts and mobilization of sulfide oxidation products). Estimated reservoir water quality (pH 3.71; 131 mg/L eq. $CaCO_3$ of acidity; and 307 mg/L of sulfate) mostly fails to comply with water guidelines, showing conditions similar to the nearby acidified Sancho Reservoir. In fact, the planned reservoir would receive more (~24.0%) acidity load than the Sancho Reservoir, proving its potential acidification after construction. Due to the severe pollution by AMD, decision makers should prioritize reclamation of the Odiel River basin before completing the Alcolea Reservoir, ensuring adequate water quality for end users.

1. Introduction

The availability of water is critical for economic development of territories, serving not only drinking water demands but also supporting agriculture, industry, and recreational activities. The spatiotemporal variability of solute export from catchments strongly influences water quality and the ecological integrity of downstream aquatic systems (Musolff et al., 2015). Such variability arises from natural processes, including chemical weathering and climatic conditions, but is often exacerbated by anthropogenic activities such as agricultural practices, wastewater discharge, industrial operations, and, notably, mining (Lottermoser, 2010). When these activities occur within river basins, they may lead to the mobilization of pollutants, potentially worsening water quality. In the case of mining, acid mine drainage (AMD) processes represent one of the most severe pressures on water resources globally, leading to increased loads of acidity, sulfates and potentially toxic elements downstream (Nordstrom, 2011; Olías et al., 2024). This problem is particularly acute in arid and semi-arid regions (Anawar, 2013), where limited water availability heightens the vulnerability of aquatic ecosystems and restricts the safe use of water for both human consumption and economic activities.

In this sense, the southwest of Spain, with dry-Mediterranean climate, faces multiple challenges related to water degradation and availability. Historical mining activities in the Iberian Pyrite Belt (IPB) have left a large-scale legacy of environmental liabilities (e.g., open pits, mine adits, tailings, sulfide-rich wastes, etc.) (Olías et al., 2024). AMD is constantly being produced in this area, with long-term dynamics (Younger, 1997), delivering large amounts of acidity and pollutants into the receiving water bodies, which deleterious effects have been widely documented, mainly in the Odiel and Tinto river basins (Olías et al., 2024). Additionally, low or non-existent natural neutralization capacity of the IPB rocks enhances the persistent transport of acidity from

* Corresponding author.
E-mail address: jonatan.romero@dct.uhu.es (J. Romero-Matos).

https://doi.org/10.1016/j.envpol.2026.128517
Received 5 February 2026; Received in revised form 29 April 2026; Accepted 3 June 2026
Available online 6 June 2026

sources towards the Atlantic Ocean (Nieto et al., 2013). On the other hand, recurrent droughts in the region, exacerbated by climate change (Arnell and Gosling, 2013), are limiting water availability. Lack of water resources, concomitant with AMD-derived degradation, poses a grave risk to the development of the region, particularly the local agricultural berry-based economy (Jurado-Almonte and Díaz-Diego, 2022). Furthermore, excessive groundwater extractions for irrigation purposes from the surroundings of the Doñana World Heritage Site (Huelva) are threatening this unique ecosystem (Camacho et al., 2022). As such, the management of AMD-impacted rivers in SW Spain must prioritize reclamation to meet water resources needs, complying also with European Water Framework Directive objectives (European Council, 2000).

To satisfy irrigation demands, the Alcolea Dam is projected to regulate the Odiel River, with 246 hm^3 of storage capacity, right after the confluence of the Oraque and Odiel rivers, the main tributaries of the basin (Fig. 1). The water quality of this reservoir has been a contentious issue since the inception of the project (Olías et al., 2011, 2024), owing to the high levels of acidity and metal pollution in its tributaries (pH

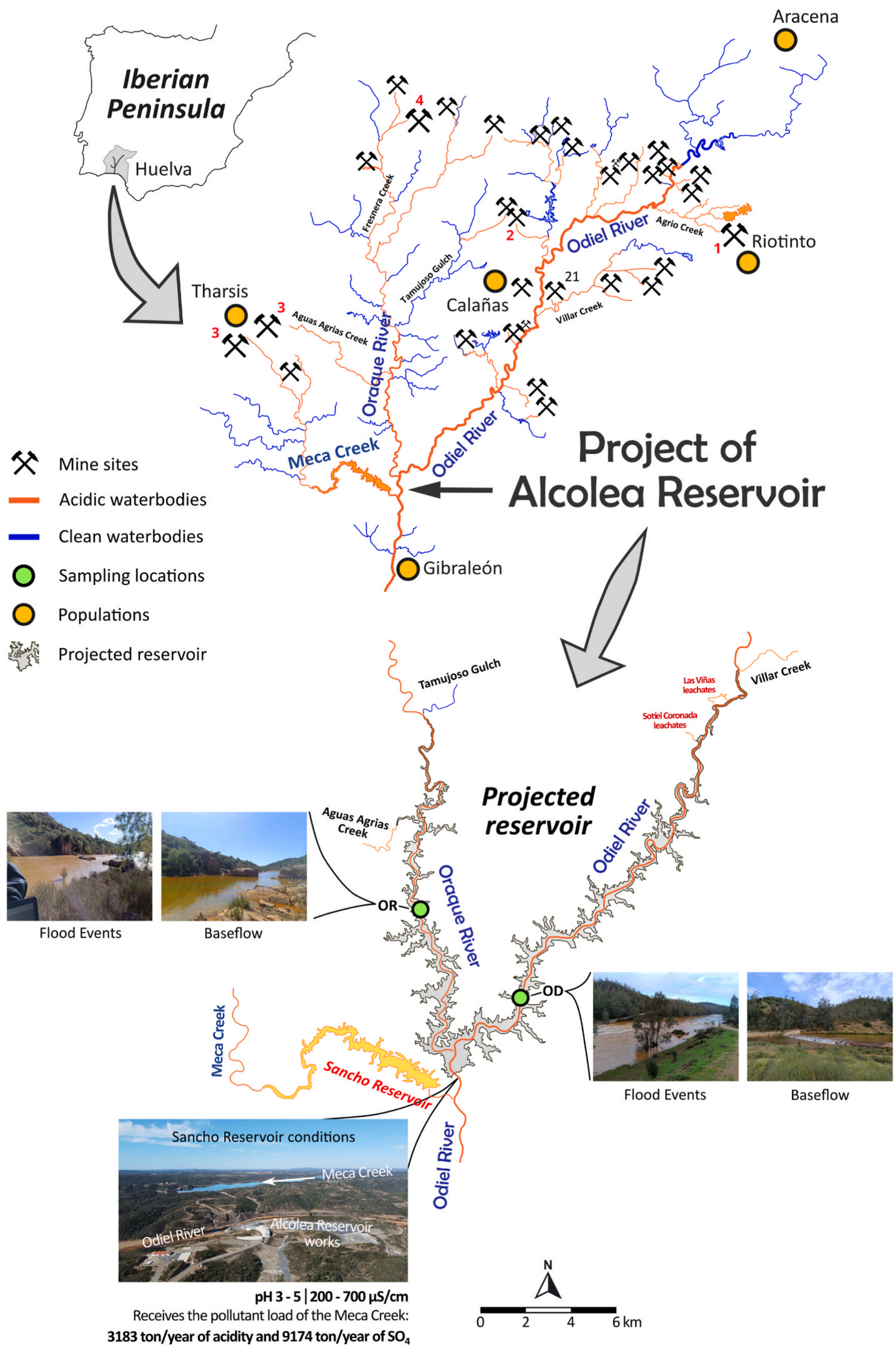

Fig. 1. Odiel River basin location map, including the main mines sites producing AMD, and the AMD-affected watercourses (37% of the total basin; Sarmiento et al., 2009). The monitoring points at the Odiel (**OD**) and Oraque (**OR**) tributaries are shown along with the projected flooded area of the Alcolea Reservoir. Flow variability is presented as images taken at both sites. As reference points, see the concrete bridge/dam over the Odiel River (used as regular section for manual gauging) and the demolished bridge in the Oraque River. Red numbers show locations of mine sites cited in text: 1. Riotinto Mines; 2. La Zarza Mine; 3. Tharsis Mines: and 4. San Telmo Mine. Photo source: Juan Carlos Toro (El País newsletter). (For interpretation of the references to colour in this figure legend, the reader is referred to the Web version of this article.)

3.18 and net acidity of 489 mg/L eq. $CaCO_3$ under average flow conditions; Romero-Matos et al., 2026). The project design assumes an improvement in water quality resulting from pollution dilution during flood events, and subsequent precipitation and sedimentation within the reservoir (ACUAES, 2010), without rigorous evidence. However, the nearby Sancho Reservoir (Fig. 1), acidified (pH ~3.5) by inputs from the Tharsis Mines (Cánovas et al., 2016a), provides a contrasting example. Despite being solely used for industrial purposes (cooling), the water still requires prior neutralization treatment to prevent pipe corrosion. Therefore, it may represent an analogue of a potential future acidification scenario for the Alcolea Reservoir if water quality is not adequately controlled. Previous works based on historical data or systematic sampling (weekly and monthly frequency) (e.g., Olías et al., 2011, 2024) concluded that the water would not be suitable for any use, yet, the authors declared that these sampling methods failed to record the sharp hydrochemical variability that takes place during intense rainy events, thereby, their results could be biased. As pointed out by Nieto et al. (2013), systematic samplings mislead pollutant loads estimations in Mediterranean climate watersheds as they often missed critical data related to rainfall events, such as "flush" effects (Cánovas et al., 2008; Nordstrom, 2011), neutralization and dilution of acidity (Sánchez-España et al., 2005; Newman et al., 2025), and increased conservative constituents loads (Byrne et al., 2020; Romero-Matos et al., 2026).

Currently, the project remains halted, with approximately 25% of the construction completed (Fig. 1). However, strong sociopolitical pressure driven by increasing water demand and the deterioration of Doñana have prompted the decision to imminently resume construction prior to a comprehensive basin-scale remediation of mining pollution, thus, leaving persisting uncertainties regarding the final water quality. In this context, the objectives of the present study are: (1) to elucidate the spatiotemporal heterogeneity in the acid generation mechanisms and rainfall response from the different mining districts in the Alcolea Reservoir tributaries (i.e., the Odiel and Oraque rivers) through high resolution samplings during a whole hydrological year; (2) to quantify the pollutant loads potentially delivered to the projected reservoir, accurately accounting for rainfall-induced flow variability and associated effects; and (3) to predict and evaluate the suitability of the resulting reservoir water quality for intended purposes. Previous studies have targeted AMD effects in existing reservoirs or lakes (Nordstrom et al., 1999; Igarashi and Oyama, 2000; Munk and Faure, 2004; Cánovas et al., 2016a), but to the best of our knowledge, this is the first work to accurately assess the acidification potential of a proposed reservoir in a complex basin severely polluted by AMD (Olías et al. 2011, 2024).

2. Methodology

2.1. Sampling methods

Two sampling sites were established within the Odiel and Oraque rivercourses, the main tributaries of the Alcolea Reservoir (Fig. 1), just upstream the reservoir dam. These sites were selected for their representativeness as the water that would be stored in the reservoir. The Odiel River (OD) site, with a drainage area of 1050 km^2, receives discharges from most of the mining complexes within the Odiel sub-basin (e.g., Riotinto Mines and La Zarza Mine), while the Oraque River (OR) site (574 km^2) collects AMD from mines located in the upper part of the Oraque sub-basin (e.g., Tharsis Mines and San Telmo Mine) (Fig. 1). A review of main hydrological, meteorological and geological characteristics of the Odiel river basin (Odiel and Oraque sub-basins) can be seen in Olías et al. (2024).

A high-resolution sampling (HRS) was performed during the hydrological year 2023/24 using Teledyne ISCO 6712 autosamplers, equipped with 24-bottle containers, polyethylene outlet pipes and pressure transducers (750 Area Velocity Flow Module) (Figure SM1). Samples were collected using a peristaltic pump, with a programmed purge to prevent cross-contamination. Sampling bottles were prewashed with 10% (v/v) HNO_3 and rinsed with Milli-Q water prior use. The sampling frequency varied from 1 to 24h depending on weather forecast, with shorter intervals during flood events and longer during dry periods. Additionally, manual samples were taken at the start of each autosampler sequence (Table SM1 and SM2). A total of 1396 samples were taken (684 at OD and 712 at OR); however, according to rainfall-induced hydrochemical variations (i.e., electrical conductivity ±20%), only 164 of OD and 158 of OR were selected for analysis.

The selection criterion is based on multiple previous studies conducted in the IPB, where a strong and recurrent relationship has been observed between most metals concentration and EC in AMD-affected rivers (Sánchez-España et al., 2005; Galván et al., 2021; Olías et al., 2024). In this context, EC has consistently proven to be a reliable proxy for the overall dissolved load and associated metal concentrations. However, first flush events may exhibit more complex hydrogeochemical dynamics; therefore, particular attention was paid to flood events occurring after the dry period, when such effects are expected to occur (Cánovas et al., 2012).

Physicochemical parameters (i.e., pH, electrical conductivity (EC), redox potential (ORP) and temperature) were measured in all samples using previously calibrated multiparameter probes (Hanna Intruments HI 9025 and HI 9033). Calibration was conducted daily prior to fieldwork and verified throughout the day using standard solutions for pH (4.01, 7.00 and 10.01), EC (84 μS/cm, 1413 μS/cm and 12.88 mS/cm), and ORP (220 mV and 468 mV). Water samples were stored in polyethylene bottles after filtration with cellulose nitrate filters (0.45 μm), acidified to pH < 2 with ultrapure HNO_3 and subsequently refrigerated at 4°C until analysis. Alkalinity was also determined by titration (CHEMetrics Total Titrets) for samples with pH > 4.5. Water level (m) was recorded every 15 min at each site via pressure transducer. Streamflow measurements were conducted using a flow meter (Global Water FP111) in a regular section at OD (Fig. 1). Channel geometry and water depth at OR made flow measurements technically unfeasible at this site.

2.2. Analytical methods

Samples were analyzed at the Central Research Services of the University of Huelva. Major elements were determined by Inductively Coupled Plasma–Optical Emission Spectroscopy (ICP-OES; Jobin Yvon Ultima 2). For the purposes of this study, only the most relevant elements associated with AMD processes were considered (i.e., Fe, Al, S, Mn, Cu, and Zn). Analytical precision was assessed through triplicate measurements,

yielding errors <5%. Blanks were included in each analytical sequence, with measured concentrations below detection limits. Analytical accuracy was verified through certified reference materials (NIST-1640). Sulfate concentrations were calculated from sulfur (S) concentrations, assuming negligible contributions from other sulfur species (Reisman et al., 2007). This assumption was validated using the geochemical modeling code PHREEQC v3.7 (Parkhurst and Appelo, 2013), which was also employed to evaluate the QA/QC of the dataset, particularly the charge balance, which indicated errors <10%, with most samples falling within ±5%. Whole dataset is available on Supplementary Material (Tables SM1 and SM2).

2.3. Rainfall and flow calculations

Based on its proximity, local rainfall data were obtained from two weather stations located in each sub-basin, "El Campillo" rain gauge station, close to the Riotinto mines within the Odiel sub-basin, and "Alosno" station in the proximities of Tharsis mines in the Oraque sub-basin. These two mining districts are considered the main sources of AMD in the respective tributaries feeding the Alcolea reservoir (Galván et al., 2016; Romero-Matos et al., 2026). Therefore, it is expected that variations in rainfall within these areas would exert the most pronounced influence on local hydrochemistry, justifying the selection of the aforementioned rainfall stations. Local rainfall will be represented along streamflow. Additionally, mean annual precipitation at basin scale was calculated using 11 weather stations.

Given the lack of gauging stations withing the basin and recurrent malfunctioning of existing ones (Romero-Matos et al., 2026) a stage-discharge relationship was developed at the OD site by correlating manual discharge measurements with corresponding water levels across a representative flow range (0.001-16.3 m^3/s; n = 7). Two rating equations were derived for water depths above and below 1 m (r^2 = 0.99) (Fig. SM2) and subsequently applied to the complete water-level record, including flood events (Table SM3). Validation against continuous discharge data from the Sotiel Coronada station, located 13.6 km upstream, yielded a correlation of $r^2 = 0.70$ (Table SM3), with deviations attributed to hydrological time lags and/or spatially variable rainfall. Flow estimations at the OR site were obtained by scaling OD discharge series using the basin-area ratio (574/1050 km^2) and establishing a rating curve based on events exhibiting comparable hydrological responses between sites. Hence, two regression models were obtained for depths above and below 1.90 m (R^2 = 0.92 and 0.75) (Fig. SM3). Note that OR flow estimations may have higher uncertainty inherent to the basin-area ratio approach. Estimated OR discharge values are provided in Table SM4.

2.4. Assessment of the potential reservoir pollution

The net acidity was estimated using the original formula proposed by Kirby and Cravotta III (2005), which includes both proton acidity relative to pH and metal acidity related to the hydrolyzable metals (Fe, Al and Mn), modified to consider other important hydrolyzable elements such as Zn and Cu (Eq. (1)) (Romero-Matos et al., 2026). This parameter is a key indicator of the potential impact of AMD on the reservoir, showing whether stored waters can neutralize the acidity supplied, or will evolve towards strongly acidic and metal-rich conditions. In this calculation, total dissolved Fe was operationally assumed to be Fe(II), as Fe speciation was not determined analytically. Therefore, net acidity values should be regarded as conservative estimates, since any contribution from Fe(III) hydrolysis would increase the calculated acidity. An approximation is calculating Fe speciation based on PHREEQC (see Supplementary Methods); however, its estimation is subject to significant uncertainty (Nordstrom, 2011; Romero-Matos et al., 2026). As a result, the actual net acidity, and particularly the net acidity load, may be higher than, or at least comparable to, the values reported here.

$$\text{Net Acidity [mg/L eq. CaCO}_3] = 50045 \cdot \left(3C_{Al} + 2C_{Fe} + 2C_{Mn} + 2C_{Zn} + 2C_{Cu} + 10^{-pH}\right) - \text{Alk} \qquad \text{Eq. 1}$$

where Cx is the molar concentration of Al, Fe, Mn, Zn and Cu (mol/L), and Alk is the alkalinity concentration (mg/L), although all measurements were below detection limit (<10 mg/L eq. $CaCO_3$).

Note that, although Fe and Al are the dominant contributors to acidity under the acidic conditions prevailing in the Odiel-Oraque-Alcolea system, the contribution of other hydrolyzable metals such as Cu, Zn, and Mn to operational net acidity within the reservoir is likely negligible, as the pH conditions required for their hydrolysis are not reached (Cánovas et al., 2016a; Olías et al., 2024). Nevertheless, these elements have been included in the modified formula for two reasons: 1) comparison with other AMD-reservoir (i.e., Sancho Reservoir); 2) due to their relevance under water treatment scenarios (proposed in Supplementary Methods), where pH is deliberately increased and their hydrolysis can contribute to overall acidity and buffering processes.

The dissolved pollutant loads delivered by Odiel and Oraque rivers were estimated using the flow-weighted average concentration method, as described by Olías et al. (2006). This approach provides more representative monthly averages, by assigning greater weight to high discharge periods, when reservoir storage is maximized. Compared to previous studies, this method offers higher resolution, since earlier assessments, mostly technical reports, often overlooked flood events (ACUAES, 2010; CEDEX, 2011; Olías et al., 2011; Olías et al., 2024), relied on limited data (Cánovas et al., 2012), or depended exclusively on modeling or concentration-discharge relationships (Galván et al., 2016).

To explicitly account for uncertainty in the reported loads, 95% confidence intervals (CI) were calculated for annual estimates using a flow-weighted approach and a normal approximation (z = 1.96), which is justified by the large number of samples (n > 100) supporting the annual calculations and the resulting asymptotic normality of the weighted mean (Gatz and Smith, 1995; Singh et al., 1999; Helsel et al., 2020). Finally, a sensitivity analysis was conducted using the lower and upper bounds of the annual confidence intervals, in order to evaluate how uncertainty in load estimates may influence the assessment of water quality conditions in the reservoir.

3. Results and discussion

3.1. Hydrological context and discharge variations

The rainfall distribution throughout the hydrological year 2023/24 was markedly irregular, recording short but intense precipitation events during the wet season (from October to March) (Figs. 2 and 3). Mean annual precipitation in the basin is 700 mm (n = 11) which is within average annual values (i.e., 1000 mm to 500 mm in the northern and southern parts of the basin, respectively; Olías et al., 2024), considering the monitored period as an average representation of interannual variations. Generally, the Odiel and Oraque rivers show rapid flow responses to rainfall events (Fig. 3ab) due to the low permeability of the materials outcropping in the drainage basin (Olías et al., 2024) (e.g., volcano-sedimentary rocks, shales, quartzites and other hard-rock materials). Furthermore, centuries of mining disturbance have created extensive man-made permeable pathways (e.g., adits, shafts, blast-induced fractures), effectively shortening subsurface flow paths and leading to the extremely rapid hydrological responses observed. The progressive increase in catchment soil moisture during persistent rainfall events leads to high river flows reached with lower rainfalls amounts (Olías et al., 2006). This trend will generally have significant implications for pollutants transport, producing peak loads even with minor precipitation events late into the wet period, as shown in the following sections. Comparatively, the Odiel River contributes a higher annual discharge to the Alcolea site than the Oraque tributary (Fig. 2), with respective contributions of 183 and 56.5 hm^3 recorded during the 2023/24 hydrological year, consistent with the larger drainage area of the former and local climatic influences (Galván et al., 2016).

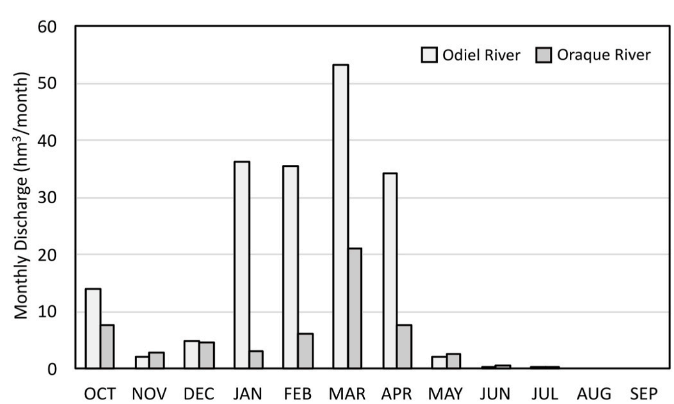

Fig. 2. Monthly discharge contribution of the Odiel and Oraque rivers to the Alcolea Reservoir during the hydrological year 2023/24.

Figure SM4 shows the recorded discharges at both points, as well as the frequency with which the rivers reach or exceed these flow rates. After the rainy season, the flow gradually decreases until the river almost dries up in summer.

3.2. Hydrochemical variations

Basic statistics of the measured parameters, flow calculations and analytical results are shown in Table 1. The whole dataset is available is Supplementary Material (Tables SM1 and SM2). Because of the multiple AMD inflows within the Odiel and Oraque sub-basins (Sarmiento et al., 2009; Cánovas et al., 2012; Romero-Matos et al., 2026), both rivers

remain mostly acidic throughout the entire monitored period, with mean pH values of 3.78 and 3.42, and mean acidity of 575 and 278 mg/L eq. $CaCO_3$ (Table 1), respectively. No alkalinity values were recorded, showing the strong AMD affection. Only during large flood events, such as those at the end of March (Figs. 2 and 3ab), pH values were close to neutrality (maximums of 6.08 at OD and 6.19 at OR; Fig. 3cd and Table 1) and acidity showed its minimum value (i.e., 1.82 mg/L eq. $CaCO_3$ at OD and 2.16 mg/L eq. $CaCO_3$ at OR). Interquartile ranges (IR) for EC were 0.64-1.95 mS/cm at OD and 0.54-1.16 mS/cm at OR, which indicates higher sulfate and metal concentrations in the former river. Generally, pH and EC values showed sharp fluctuations as a response to rainy events, when flow increments lead to pH peaks and EC minimum values due to runoff dilution and neutralization effects (Nieto et al., 2013; Olías et al., 2024).

However, during the rising and falling limbs of flood events, particularly those preceded by prolonged dry periods, the behavior of physicochemical parameters becomes considerably more complex (Figs. SM5 and SM6). Following summer, and coinciding with a major rainstorm at the end of Oct.-23, a pronounced flush effect was recorded at both points (Fig. 4, SM5 and SM6). During the rising limb, pH increased slightly from 3.10 to 4.08 at OD, and from 2.60 to 4.00 at OR, whereas EC decreased from ~4.80 mS/cm in both rivers to 0.53 at OD and 1.90 at OR (Figs. SM5 and SM6). This initial attenuation was likely driven by runoff dilution and transient hydrochemical buffering (Sarmiento et al., 2009; Cánovas et al., 2012), and was subsequently followed by the arrival of flushed mineralized waters in one or more chemically distinct pulses. At OD, pH dropped to 3.16 and EC increased to 1.94 mS/cm around 14-15 h after the onset of the discharge rise, followed by the arrival of less mineralized waters (Fig. SM5). Approximately 19 h after, a second and much more intense pulse was recorded, causing a sharp drop in pH to 2.58 while EC peaked at 5.06 mS/cm (Fig. SM5). On the contrary, at OR only one pulse was identified, occurring 6-7 h after the initial rising limb, decreasing pH to 2.63, while EC reached 4.83 mS/cm (Fig. SM6). These flush responses likely reflect the dissolution of evaporitic salts, which act as temporary solid-phase storage of acidity and metals during dry periods, together with the mobilization of concentrated AMD waters stored in riverbanks, mine sites, and pore fluids within spoil heaps; processes previously recognized as major controls on solute export in mining-impacted basins (Keith et al., 2001; Cánovas et al., 2008, 2017; Nordstrom, 2009; Petach et al., 2021).

In the case of OD, the occurrence of two distinct pulses may be attributed to the following hypothesis. In the IPB, summer evaporation leads to the accumulation of highly soluble sulfate salts such as

Table 1
Descriptive statistics of the high-resolution sampling in the Odiel and Oraque rivers during the hydrological year 2023/24. S.D.: standard deviation; P25 and P75: percentiles 25th and 75th. *Note that Oraque flow have been estimated based on basin-area ratio, with inherent uncertainties, while Odiel flow is based on calculated rate curve.

		Odiel River (OD)							
		n	Min.	Max.	Mean	Median	S.D.	P25	P75
pH		684	2.58	6.08	3.78	3.62	0.62	3.25	4.27
EC	mS/cm	684	0.15	5.54	1.43	0.94	1.23	0.64	1.95
Eh	mV	684	411	804	697	700	63.0	666	747
Flow	m^3/s	16106	0.001	350	10.1	1.53	30.7	0.43	6.05
Net Acidity	mg/L eq. $CaCO_3$	164	1.82	2485	575	315	586	147	793
Major Constituents (mg/L)									
Al		164	0.05	356	86.2	45.7	89.4	22.3	119
Ca		164	8.53	338	92.0	47.3	98.1	31.7	95.8
Cu		164	0.05	24.7	6.02	4.20	5.01	2.06	9.54
Fe		164	0.05	64.2	3.70	1.65	7.33	0.42	4.01
K		164	1.16	30.9	4.60	2.68	4.62	1.83	4.28
Mg		164	6.66	457	129	67.6	130	39.4	172
Mn		164	0.39	63.4	16.8	8.11	18.0	4.30	21.3
Na		164	7.38	122	31.4	17.4	31.8	14.2	23.7
Sulfate		164	46.7	4382	1231	643	1242	356	1632
Zn		164	0.15	68.6	18.9	10.4	18.8	5.47	25.9
		Oraque River (OR)							
		n	Min.	Max.	Mean	Median	S.D.	P25	P75
pH		712	2.21	6.19	3.42	3.31	0.69	3.09	3.64
EC	mS/cm	712	0.15	5.79	1.29	0.77	1.35	0.54	1.16
Eh	mV	712	410	827	707	714	66.3	684	753
Flow*	m^3/s	15943	0.001	114	2.85	1.52	7.95	0.99	2.50
Net Acidity	mg/L eq. $CaCO_3$	158	2.16	1885	278	121	386	69.6	212
Major Constituents (mg/L)									
Al		158	0.05	220	29.3	12.7	40.4	7.92	24.7
Ca		158	8.75	246	49.3	27.0	58.6	22.0	37.3
Cu		158	0.05	16.8	2.45	1.32	2.60	0.82	2.49
Fe		158	0.05	162	20.0	5.94	36.8	1.37	11.5
K		158	1.18	58.9	4.59	3.04	6.42	2.03	3.96
Mg		158	7.11	359	69.9	32.6	88.9	25.5	53.9
Mn		158	0.35	54.4	5.81	2.70	8.31	1.60	4.11
Na		158	9.62	172	33.7	20.6	38.4	16.2	26.8
Sulfate		158	49.5	3571	654	281	866	213	513
Zn		158	0.44	83.5	11.7	4.85	15.5	3.25	9.63

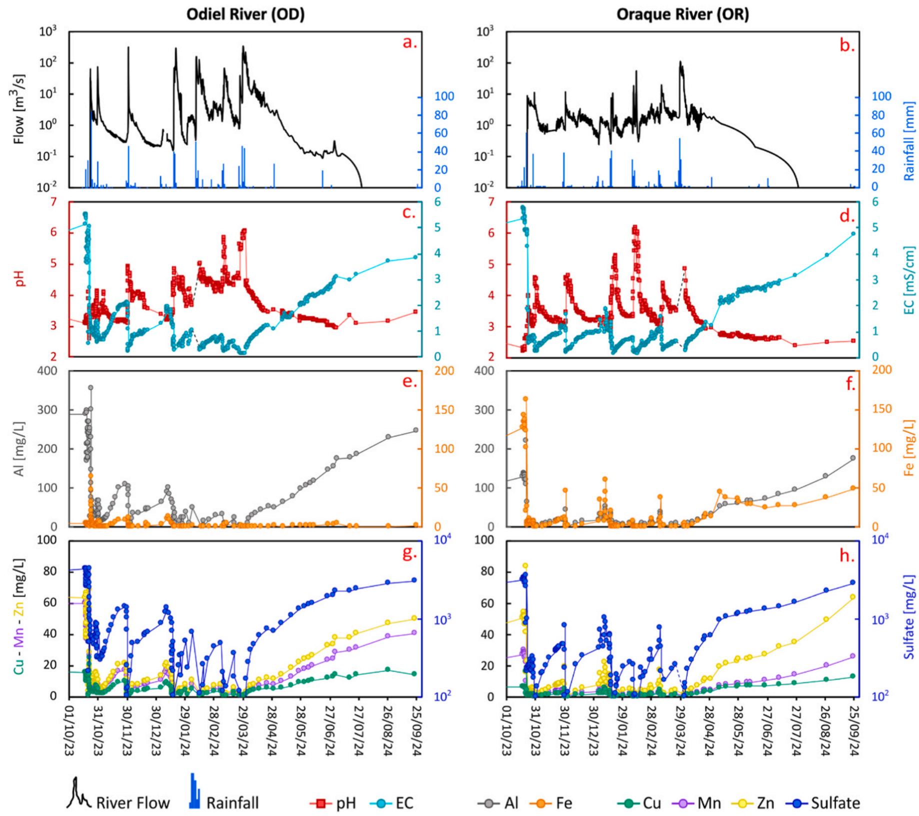

Fig. 3. a. Hydrograph of the Odiel River at OD and rainfall collected at “El Campillo” pluviometric station (Odiel sub-basin). **b.** Hydrograph of the Oraque River at OR and rainfall collected at “Alosno” pluviometric station (Oraque sub-basin). Variations of pH and electrical conductivity (EC) at OD (**c**) and OR (**d**). Evolution of dissolved concentrations of Al-Fe at OD (**e**) and OR (**f**), and Cu-Mn-Zn-Sulfate at OD (**g**) and OR (**h**). Dash lines on **c** and **d** represent data gaps.

melanterite, copiapite, coquimbite and/or jarosite along channel margins (e.g. Sánchez-España et al., 2005). These minerals exhibit markedly different dissolution kinetics and acid-generating capacities, while melanterite dissolves rapidly, releasing Fe(II) and SO_4 and producing an early conductivity peak, copiapite, coquimbite and jarosite, enriched in Fe(III), dissolve more slowly but contribute more directly to acidity generation and sustained metal release (e.g., Blowes et al., 2003; Jamieson et al., 2005). The dissolution of AMD-related sulfate salts and other secondary minerals may involve mineral-specific and kinetically complex release patterns, which is known to control the temporal evolution of pH and metal concentrations during first-flush events at source scales (Cánovas et al., 2016b; Caraballo et al., 2016; Basallote et al., 2019). However, such fine-scale behavior is unlikely to remain individually resolvable at the scale of flood response in downstream sections (Cánovas et al., 2008, 2017). Another possibility is the sequential activation of hydrogeochemically different but related AMD reservoirs, likely involving an initial flush of rapidly connected superficial salts and shallow acidic waters, followed by the delayed mobilization of more internally stored, highly mineralized waters and/or sub-surface secondary mineral accumulations.

The temporal discrepancies between acidity pulses at both points highlights the contrasting characteristics of each sub-basin and, particularly differences in the location, connectivity, and relative dominance of AMD source areas (Fig. 1). The rapid arrival of the pulse at OR may be attributed to the short travel time and strong hydrological coupling with Aguas Agrias Creek, which drains acidic leachates from the Tharsis mining district, one of the major AMD sources in the Oraque sub-basin (Fig. 1) (Galván et al., 2016; Moreno-González et al., 2022; Romero-Matos et al., 2026). In contrast, the two-pulse response observed at OD suggests the progressive activation of distinct AMD reservoirs within one or a few dominant upstream source areas. Given its dominant contribution to AMD loading at OD, the Riotinto Mining Complex (>70% contribution; Galván et al., 2016; Romero-Matos et al., 2026) is the most plausible source responsible for both pulses, or at least for the second and most pronounced contaminant pulse (Cánovas et al., 2008). The delayed arrival of the pulses at OD (>14h from discharge onset), compared to the sole early pulse at OR (~6h), further supports the association of flush events with the primary AMD sources previously mentioned, given the distance of both mine sites from their respective monitored points (Fig. 1). A rough estimation of travel time based on average flood velocities (e.g., 1.24 m/s measured on March flood event) could also help discriminate between a local origin (i.e., channel scour and in situ salt dissolution) and an advective input from upstream mine drainage (e.g., Riotinto Mines). Thus, the estimated travel time is 11-13h, approximately coinciding with the time elapsed between the discharge onset and the recording of the first pulse.

Furthermore, the temporal offset between pulses at OD may be associated with the presence of multiple types of AMD sources within the Riotinto mine area (i.e., spoil heaps, adits, tailings, settling ponds, etc.), which likely host metal-acidity compartments with contrasting accessibility, storage behavior, and hydrological response (Cánovas et al., 2008). Such complex hydrodynamics are poorly understood (e.g., different water routing through mines wastes and underground workings) (Younger, 2000; Sáinz et al., 2002; Nordstrom, 2009; Cánovas et al., 2016b; Caraballo et al., 2016), highlighting the need for site-by-site case studies. Importantly, this interpretation does not exclude the simultaneous flushing of salts and acidic waters from multiple upstream mine sites throughout the event (e.g., La Zarza Mine, San Telmo Mine, etc.) (Fig. 1). Rather, it suggests that such distributed contributions may remain partially masked at the downstream section due to dilution by flood waters, in-stream hydrochemical buffering, and catchment-scale mixing, becoming clearly identifiable only when contaminant release from dominant source areas exceeds the attenuation capacity of the fluvial system. Additionally, particulate matter should also be analyzed to evaluate their potential metal transport during flush events (Kimball et al., 2007; Cánovas et al., 2012, 2017). As the temporal acidity storage is progressively depleted with subsequent rainfall events, freshwater dilution processes become increasingly dominant in the basin.

Main AMD constituents (i.e. Al, Fe, Cu, Zn, Mn and sulfate) show similar patterns as EC (Fig. 3, SM5 and SM6). Concentrations are normally diluted when freshwater contribution increases (i.e., discharge peaks), followed by a recovery due to the arrival of more mineralized waters from AMD sites (Sarmiento et al., 2009; Cánovas et al., 2012; Newman et al., 2025). Sharp increases in concentrations are observed during some flood events due to flush effects (Fig. 3, Fig. SM5 and SM6), with maximum values at the end of October (e.g., OD: 64.2 mg/L of Fe, 356 mg/L of Al and 4.38 g/L of sulfate; OR: 162 mg/L of Fe, 220 mg/L of Al and 3.57 g/L of sulfate). High loads of Fe and Al are released to watercourses during these events, playing an important role in buffering the pH by hydrolysis (Nordstrom, 2011; Sánchez-España et al., 2011) despite the arrival of freshwaters, hence, both rivers remain mostly acidic (pH < 5) until acidity is consumed.

Overall, the hydrochemical conditions of both rivers, and thus the waters feeding the projected Alcolea reservoir, seem to be controlled by the balance between the incoming acid load, which fluctuates throughout the year, and the limited attenuation and neutralization capacity, which is most effective during high-flow periods (Fig. 4c). Notable differences in constituent concentrations distinguish the two rivers: OD exhibits substantially higher sulfate (IR 356-1632 mg/L) and metal concentrations (Al, Cu, Mn, Zn) than OR (Table 1), whereas Fe concentrations are higher in OR (IR 1.37-11.5 mg/L). This may be attributed to its proximity to the Tharsis mines and the reduced mixing with cleaner tributaries, as AMD from the Tharsis district may preserve a higher $Fe(II)/Fe_{Total}$ ratio, while the upper Oraque sub-basin lacks significant alkaline tributaries (compared to Odiel alkaline headwaters; Olías et al., 2024), thereby kinetically limiting Fe oxidation and precipitation/retention. In contrast, despite the higher overall contaminant load transported by OD, the longer flow path and more intense natural attenuation processes likely promote more effective natural Fe removal through oxidation-hydrolysis and secondary mineral precipitation (e.g., schwertmannite/jarosite formation), resulting in lower dissolved Fe concentrations at the downstream monitoring point. These conditions could also explain the lower pH at OR (IR 3.09–3.64), where Fe hydrolysis may exert a strong control, while higher pH at OD (IR 3.25–4.27) is more influenced by Al (and minor Fe) hydrolysis (Sánchez-España et al., 2011), consistent with its greater distance from AMD sources. Late-year conditions in both rivers show increasing solute concentrations and declining pH as freshwater inputs decrease and AMD dominance, evaporation, and reconcentration intensify.Table 2.

3.3. Water quality assessment

In order to evaluate water quality during the year 2023/24, samples have been plotted on a modified Ficklin diagram (Ficklin et al., 1992). Water quality fields have been established based on uses and recommendations from regulatory entities (irrigation waters according to FAO: Ayers and Westcot, 1985; and human use according to WHO and EU: World Health Organization, 2022; European Council, 2020). In addition, average values for reservoirs in the region have been represented, both those affected by AMD (Sancho, Olivargas, and Andévalo) and those unaffected (Jarrama and Corumbel) (Olías et al., 2011, 2024) (see data in Table 2 and reservoir locations in Fig. SM7).

The water quality recorded did not comply with guidelines for irrigation and human use, with all samples out of thresholds pH ranges. Although it remains possible that during flood events, exceeding those observed this year, pH values > 6.5 could be reached (Olías et al., 2024). Maximum concentrations guidelines are based on the sum of individual concentration limits for Al, Cu, Fe, Mn and Zn (Tables 2 and Tables SM5) - main AMD metals producing acidity. Most samples fail to comply with concentration limits, however, an improvement in conditions lead by dilution and neutralization effects during high flows is observed (Fig. 4ac). Only 3.66-7.32% (n = 164) of samples at OD and 6.45-21.9% (n = 158) at OR met recommendations, depending on the specific water guideline (i.e., WHO, EU or FAO). These differences between tributaries are mainly attributed to the higher degree of AMD pollution on the Odiel River, as mentioned in the previous section. Both tributaries are controlled by geochemical mixing processes between AMD sources and freshwater inputs (Fig. 4b), with the relative contribution of each determining the position of the tributary water quality along a theoretical mixing line. In addition, a detailed assessment of other potentially toxic elements present in AMD waters (e.g., Ni, Co, As, Pb, Cd) (Nieto et al., 2013; Cánovas et al., 2016a; Galván et al., 2021) is necessary to evaluate their effects on reservoir water quality.

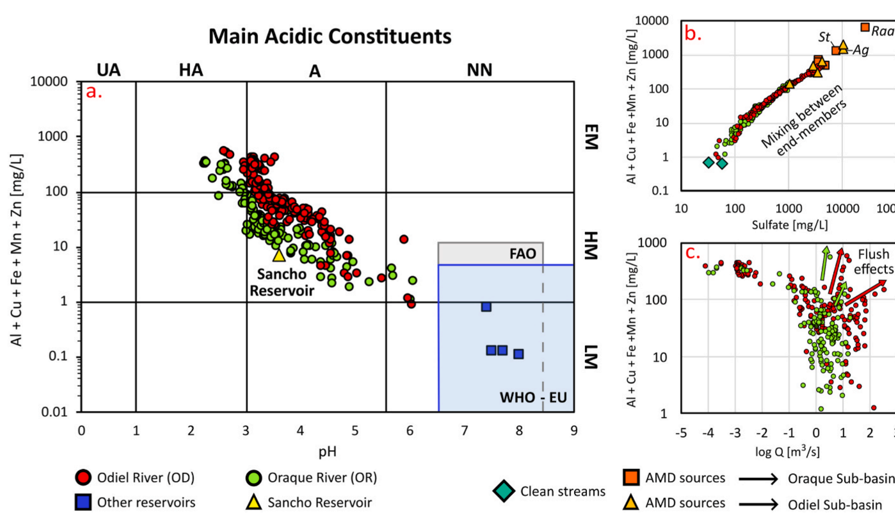

Fig. 4. **a.** Modified Ficklin Diagram of river samples collected during the year 2023/24. Mean values of reservoirs in the IPB are plotted for comparison purposes (Olías et al., 2011, 2024) (refer to). Water quality thresholds are also presented (irrigation: Ayers and Westcot, 1985; human use: World Health Organization, 2022; European Council, 2020). UA: Ultra acidic; HA: Highly acidic; A: Acidic; NN: Near neutral; EM: Extremely metallic; HM: High metallic; LM: Low metallic. **b.** Influence of sources on the Odiel and Oraque rivers hydrochemistry. Ag: Riotinto Mines; Raa: Tharsis Mines; St: San Telmo Mine. **c.** Concentration-discharge (C-Q) relationships for main dissolved AMD-constituents. Red and green arrows indicate flush effects at OD and OR, respectively. (For interpretation of the references to colour in this figure legend, the reader is referred to the Web version of this article.)

When considering endmembers - clean waters from unaffected upstream reaches and AMD sources (from Romero-Matos et al., 2026) - the hydrochemistry of OR is mainly controlled by the mixing of acidic leachates from the Tharsis Mines ("Raa" in Fig. 4b), and to a lesser extent from San Telmo Mine ("St" in Fig. 4b), with clean surface waters. In contrast, OD shows a dominant influence from AMD discharges originating in the Riotinto Mines ("Ag" in Fig. 4b). The three mine sites have been already reported as prominent sources of AMD in the Odiel basin and remediation actions should prioritize on these sites (Galván et al., 2016; Olías et al., 2024; Romero-Matos et al., 2026).

For comparison purposes, other reservoir waters in the area were also plotted in Fig. 4a (data in Table 2), including those receiving AMD inputs (i.e., Olivargas and Andévalo reservoirs). Exceptionally, the Sancho reservoir, built next to the planned Alcolea reservoir, with 48 hm^3 of water stored, exhibit acid conditions (mean pH 3.6) and high metal concentrations (Table 2) (Cánovas et al., 2016a; Olías et al., 2024), posing as a large-scale environmental liability. According to Olías et al. (2024), sulfate levels are a reliable indicator of AMD impact on reservoirs due to its nominally conservative behavior in AMD environments. The sulfate loads transported by AMD-affected tributaries to the Olivargas, Andévalo, and Sancho reservoirs are estimated at 2898, 6011 and 9174 ton/year, respectively (Grande et al., 2010; Cánovas et al., 2017; Galván et al., 2021). If normalized to reservoir average annual contribution, these values correspond to 56.8-, 50.1-, and 287-ton SO_4/hm^3, respectively. These values indicate that the Sancho is the most AMD-impacted reservoir, while Olivargas also exhibits a slightly higher sulfate enrichment than Andévalo, thereby explaining the worst conditions observed in the Sancho reservoir, and suggesting vulnerability to future acidification if AMD contributions persist in the others.

3.4. Transport of acidity and metals to the reservoir

The estimated dissolved loads of acidity and sulfate and respective flow-weighted mean concentrations are shown on Fig. 5. Monthly dissolved elements loads and mean concentrations can be consulted in Tables SM5 and SM6; related uncertainties are shown in Tables SM7 and SM8. The global flux of dissolved net acidity into the Alcolea reservoir during the monitored year has been estimated in 31247 tons eq. $CaCO_3$ ($CI_{95\%}$: ±25056 tons), of which 78 ± 3.28% comes from the Odiel River and 22 ± 3.28% from the Oraque River (Table SM6), consistent with the greater AMD impact observed in the former (Romero-Matos et al., 2026). In the case of dissolved sulfate load, a total of 73598 tons ($CI_{95\%}$: ±43782 tons) were delivered, 77 ± 2.02% from the Odiel (Table SM6). Similar relative contributions were observed in the Odiel river for most metals (83-74 ± 1.31%) (Table SM6), however, remarkable contributions of dissolved Fe loads were associated with Oraque, contributing approximately 66 ± 22.9% of the total (Table SM6), indicating that a significant portion of Fe has precipitated in upstream Odiel sections (Sánchez-España et al., 2005; Sarmiento et al., 2009), given the higher loads of other acid metals comparatively.

The relatively wide confidence intervals associated with the estimated annual loads likely reflects the intrinsic high variability of the Odiel basin hydrology-hydrogeochemistry throughout the hydrological year, when a substantial fraction of the total mass flux is controlled by episodic high-flow events, such as October or March floods (Figs. 2 and 5; Table SM6). Consequently, the reported uncertainty primarily captures natural system variability rather than limitations in sampling density.

The importance of flush events on annual loads is evident when considering that October floods only accounted between 8 ± 0.17% and 14 ± 0.13% of the Odiel and Oraque river contributions (Fig. 2; Table SM6), but strikingly produced 25 ± 3.85% of acidity load and 21 ± 1.90% of sulfate load (Fig. 5a; Table SM6) that could potentially be impounded in the reservoir during autumn floods. Monthly mean concentrations were consistently high during this period (Fig. 5cd; Table SM5) due to flush effects. This suggests that the initial reservoir volume, which is critical for the chemical evolution of the system, would already be significantly polluted from the reservoir onset. March intense rainfalls produced the highest flows (Figs. 2 and 3ab; Table SM6), with respective subsequent metal-acidity transport events.

The estimated loads for 2023/24 (i.e., 73598 ton/year SO_4) are lower than average annual loads reported by Olías et al. (2006) for 1995–2003 (e.g., 147213 ton/year SO_4), based on weekly synoptic samplings and concentration-discharge regressions, although mean annual precipitation was greater (981 mm) in that period than in 2023/24 (700 mm). Nieto et al. (2013) estimated a load of 59641 ton/year of SO_4 using a systematic sampling in 2005/06 with a mean precipitation of 637 mm, which is slightly lower (~14%) than 2023/24, along with sulfate loads comparatively lower (~19%). These values highlight that pollutant transport is strongly controlled by annual precipitation in AMD-affected watersheds. Other potential factors include the mine sites hydrological connectivity with rivers (e.g., saturated vs. unsaturated underground workings or mine wastes, open pit overflowing, transient vs. permanent leachates); rainfall distribution and antecedent dry/wet period conditions; the available stock of secondary sulfate salts and stored acidic waters; and anthropogenic disturbances (e.g., mining cessation/re-opening, remediation, reservoir construction, or accidental spills) (Sáinz et al., 2002; Cánovas et al., 2008; Runkel et al., 2016; Petach et al., 2021; Olías et al., 2024).

Based on the sulfate load estimated for the year 2023/24, the Alcolea Reservoir, with an estimated contribution of 240 hm^3, would receive ~307 ton SO_4/hm^3, around 7% more than the Sancho Reservoir (287 tonSO_4/hm^3; Cánovas et al., 2017); and would accumulate ~130 ton acidity/hm^3, about 24% more than the Sancho (99.5 ton acidity/hm^3; Cánovas et al., 2017). These results suggest that the Alcolea Reservoir could potentially experience a rapid acidification like the Sancho

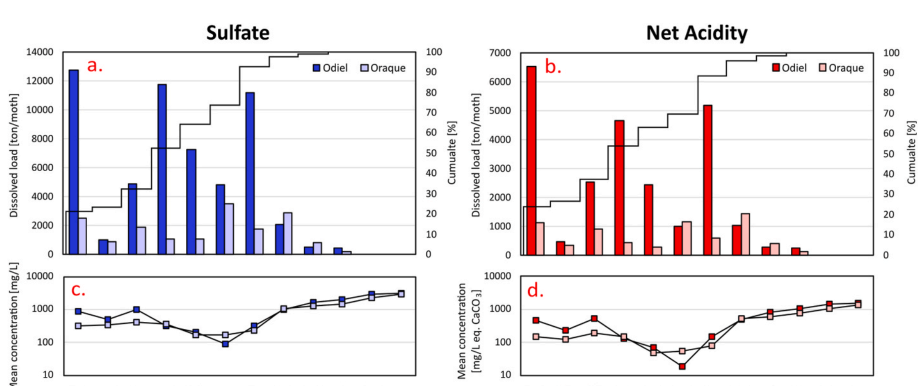

Fig. 5. Monthly sulfate (**a**) and net acidity (**b**) loads of the Odiel (OD) and Oraque (OR) tributaries of the Alcolea Reservoir, with respective contribution percent to total annual load. Refer to Fig. 2 for comparing with monthly discharge contribution. Flow-weighted mean concentrations for sulfate (**c**) and net acidity (**d**).

Reservoir. Cánovas et al., 2016a reported a shift in the Sancho pH-buffer from Al to Fe, with subsequent metal increases, within 5-6 years following the Tharsis Mines closure by rebound effect. Considering the higher acidity and sulfates fluxes observed in Alcolea tributaries, similar processes may occur over shorter timescales. Additionally, in order to account for uncertainties in load estimations, a sensitivity analysis using the lower and upper bounds of the annual confidence intervals has been conducted and can be consulted in **Supplementary Methods**.

3.5. *Estimated reservoir conditions*

Table 2 shows the water quality that the Alcolea Reservoir would store upon current conditions according to the present study (i.e., pH 3.71; 131 mg/L eq. $CaCO_3$ of net acidity; and 307 mg/L of sulfate). Methods and additional information related to this section can be consulted in **Supplementary Methods**, along with a sensitivity analysis performed for water quality estimation. Estimated water quality mostly fail to comply with water guidelines and predicts that reservoir conditions are closer to the current acidified Sancho Reservoir.

The balance between acidity and alkalinity controlling the reservoir water quality is clearly shifted towards acidification, indicating that natural attenuation processes alone are insufficient to ensure a suitable water quality (**Supplementary Methods**). Furthermore, although the treatment of reservoir water is technically feasible, it may not be cost-effective in the long term, as its sustainability largely depends on the potential and consistent economic benefits of end users (**Supplementary Methods**). Consequently, decision-makers should implement a reclamation plan for the Odiel River basin either concurrently with or prior to the construction of the Alcolea Reservoir, thereby ensuring that the impounded water procures a higher quality standard, fulfilling the requirements of the current water policy goals (European Council, 2000). Romero-Matos et al. (2026) developed a management tool to optimize economic resources for a large-scale reclamation plan in the Odiel basin, demonstrating that reductions in AMD generation would significantly improve water quality. Their results also highlight the need for a full and appropriate plan as minor restoration measures (<50% reduction of AMD generation) would be insufficient to achieve proper water goals. Given the complexity of source hydrology (e.g., point vs. diffuse sources) and heterogeneity of waste deposits at each mine site, which result in distinct geochemical signatures and pollutant dynamics, future research should focus on the detailed characterization of individual mine sites to support the design of effective remediation measures.

4. Environmental and policy implications

The finding of this study reveal that the infrastructure planned for the Odiel River basin may not meet the desired objectives at the short term, fundamentally related to regional water demands, due to poor water quality of feeding watercourses. Acidic drainages have been demonstrated to have a deleterious effect on reservoirs worldwide (e.g., Nordstrom et al., 1999; Igarashi and Oyama, 2000; Munk and Faure, 2004; Palma et al., 2015), leading to a detrimental reduction in the viable use of these water bodies. A remarkable example is the Spring Creek Reservoir, built to store the extreme acidic discharges from the Iron Mountain Mine, preventing them from entering the Keswick Reservoir (Antweiler et al., 2012; Jacobs et al., 2016). Prior to reclamation, the water quality exhibited a markedly acidic character (pH < 3), with high dissolved concentrations of metals, and Cu- and Zn-rich sediments. Furthermore, unplanned releases of acidic water into the Keswick Reservoir occurred during some high-flow events, with negative impacts downstream. Remediation measures were later implemented leading to an overall improvement, significantly reducing >95% the pollutant loads delivered to the reservoir. Although costly, the effects of reclamation efforts are well documented and have allowed authorities to greatly improve the regional water resources management. From a policy perspective, this underscores the need to prioritize preventive, source-control and treatment measures at the catchment scale, supported by long-term monitoring and management of legacy mine sites. Furthermore, research is increasingly focusing on the revalorization of treatment residues enriched in metals of economic interest, demonstrating that these residues could serve as secondary sources of critical raw materials (Macías et al., 2017; Rakotonimaro et al., 2017; León et al., 2021; 2025). This approach supports AMD remediation at its source, contributing to catchment restoration while partially offsetting treatment costs within a circular economic framework.

Without basin restoration, the use of reservoir waters for irrigation could lead to soil acidification and degradation of agricultural fields (Zhang et al., 2013). Another potential environmental risk is the occurrence of mine spills from old mining infrastructures located upstream of the reservoir. An example of these events is the mine spill occurred in the Odiel River basin in May 2017, when approximately 270,000 m^3 of acidic water stored in the La Zarza pit lake were accidently released following the rupture of a concrete plug in an old gallery connected to the pit (Olías et al, 2019; Pérez-López et al., 2025). As a result, large quantities of pollutants were rapidly discharged into the Odiel River. Upon the construction of the Alcolea Reservoir, the lack of control measures in derelict mines of the IPB may lead to other accidental spills from mine adits or tailing dams into the newly constructed reservoir. Furthermore, climate change might increase the production rate of AMD or metal mobilization due to global warming (Anawar, 2013; Manning et al., 2024), intensifying the metal transport export from mine sites (Nordstrom, 2009; Van Vliet et al., 2023) and worsening the quality of downstream waters.

Table 2
Flow-weighted mean annual concentrations resulting from the mixing of the Odiel and Oraque tributaries. Guidelines recommendations and mean values of other reservoirs located in the IPB (see Section 3.3 for explanation) are exhibited for comparison purposes. No data is represented by double dash ("–").

	pH	Al	Cu	Fe	Mn	SO_4	Zn	Net Acidity
		mg/L						mg/L eq. $CaCO_3$
Alcolea Reservoir (2023/24)								
Estimation	3.71	18.4	1.86	0.81	3.41	307	4.86	131
Guidelines recomendations								
FAO - Irrigation Waters	6.5 - 8.4	5	0.2	5	0.2	–	2	–
WHO - Human use	6.5 - 8.5	0.9	2	0.2	0.08	500	3	–
EU - Human use	6.5 - 9.5	0.2	2	0.2	0.05	250	–	–
Other reservoirs in the IPB (Mean values)								
Sancho Reservoir	3.60	4.37	0.91	0.84	2.34	184	3.06	48.8
Olivargas Reservoir	7.40	–	0.014	0.12	0.27	63.0	0.41	–
Andévalo Reservoir	7.50	–	0.005	0.05	0.04	57.0	0.03	–
Corumbel Reservoir	8.00	–	0.002	0.06	0.03	12.0	0.02	–
Jarrama Reservoir	7.70	–	0.004	0.09	0.02	11.0	0.02	–

5. Conclusions

A year-long, high-resolution investigation of the Odiel and Oraque tributaries (SW Spain) demonstrates that dissolved pollutant loads to the planned Alcolea Reservoir are predominantly governed by flood-driven hydrological dynamics. The application of flow-weighted mean concentrations, supported by intensive temporal sampling, yielded robust load estimates and reliable predictions of water-quality evolution. Data from 2023 to 2024 indicate that, in the absence of prior basin-scale reclamation, tributary waters remain severely impaired and unsuitable for any foreseen reservoir use. Persistently acidic conditions were recorded (mean pH 3.78 in the Odiel and 3.42 in the Oraque), together with elevated net acidity and sulfate concentrations that consistently exceeded regulatory thresholds, even under dilution-dominated flood conditions. The estimated annual fluxes of dissolved net acidity (~31,247 ton eq. $CaCO_3$) and sulfate (~73,598 ton SO_4) entering the reservoir were dominated (77–78%) by the Odiel River, reflecting its stronger AMD impact.

These fluxes are above (7-24%) those reported for the already acidified Sancho Reservoir, implying a high risk of rapid reservoir acidification following impoundment.

Generally, results indicate that the acidity–alkalinity balance is strongly shifted toward acidification, with natural attenuation processes insufficient to achieve acceptable water quality. Consequently, effective management must prioritize basin-scale remediation and pollution mitigation prior to impoundment, as reliance on natural attenuation or long-term active treatment would entail escalating economic costs and render the reservoir an enduring environmental and socio-economic liability. Additionally, even though intense remediation actions are implemented in AMD sources and short-term attenuation could occur after impoundment (via sediment adsorption or in-situ mineral precipitation), the long-term stability of pollution retention in reservoir sediments cannot be assumed. In fact, reservoir sediments may act as internal loading of acidity and metals to the water column, through diagenetic and redox-mediated processes or progressive changes in reservoir pH, representing an additional water quality risk, which needs to be monitored during the reservoir exploitation.

CRediT authorship contribution statement

Jonatan Romero-Matos: Writing – review & editing, Writing – original draft, Visualization, Methodology, Investigation, Conceptualization. **Laura Sánchez-López:** Writing – review & editing, Methodology, Investigation. **Rafael León:** Writing – review & editing, Methodology, Investigation. **Francisco Macías:** Writing – review & editing, Methodology, Investigation, Conceptualization. **Carlos R. Cánovas:** Writing – review & editing, Supervision, Project administration, Funding acquisition, Conceptualization. **Manuel Olías:** Writing – review & editing, Validation, Conceptualization. **José Miguel Nieto:** Writing – review & editing, Supervision, Project administration, Funding acquisition.

Declaration of competing interest

The authors declare that they have no known competing financial interests or personal relationships that could have appeared to influence the work reported in this paper.

Acknowledgements

This research was funded by the the Spanish Ministry of Science, Innovation and Universities under the research project DYNAMICO (PID2023-151504OB-I00) funded by MICIU/AEI/10.13039/501100011033; and by the European Council, 2020 Research and Innovation Programme under the I+D+ i ERA-MIN3 SuMRee project (PCI2024-153500) funded by MICIU/AEI/10.13039/501100011033, and the HydroShift project (PCI2025-167130-2). L. Sánchez-López acknowledges the "Formación de Personal Investigador" grant (PRE2021-097651) funded by MCIN/AEI/10.13039/501100011033. J. Romero-Matos is financed by a FPU program of the Spanish Ministry of Education and Vocational Training (FPU20/04441). We are deeply grateful for the assistance provided by the members of the Mineralogy and Environmental Geochemistry research group and other colleagues during the extensive fieldwork. The authors gratefully appreciate the constructive comments and suggestions from the editor Klaus Kümmerer and two anonymous reviewers. Funding for open access charge: Universidad de Huelva/CBUA.

Appendix A. Supplementary data

Supplementary data to this article can be found online at https://doi.org/10.1016/j.envpol.2026.128517.

Data availability

Data will be made available on request.

References

ACUAES, 2010. Modificación N° 1 Del Proyecto De Ejecución De Las Obras De La Presa De Alcolea. Anejo N° 18. Calidad De Aguas. Informe Técnico. Aguas de las Cuencas de España, Ministerio de Medio Ambiente y Medio Rural y Marino, p. 149. Anexos.

Anawar, H.M., 2013. Impact of climate change on acid mine drainage generation and contaminant transport in water ecosystems of semi-arid and arid mining areas. Phys. Chem. Earth, Parts A/B/C 58, 13–21. https://doi.org/10.1016/j.pce.2013.04.002.

Antweiler, R.C., Taylor, H.E., Alpers, C.N., 2012. Distribution and geochemistry of selected trace elements in the Sacramento River near Keswick reservoir. Chem. Geol. 298, 70–78. https://doi.org/10.1016/j.chemgeo.2011.12.025.

Arnell, N.W., Gosling, S.N., 2013. The impacts of climate change on river flow regimes at the global scale. J. Hydrol. 486, 351–364. https://doi.org/10.1016/j.jhydrol.2013.02.010.

Ayers, R.S., Westcot, D.W., 1985. Water quality for agriculture. In: Food and Agriculture Organization of the United Nations. Rome. https://www.fao.org/4/t0234e/T0234E00.htm#TOC.

Basallote, M.D., Cánovas, C.R., Olias, M., Pérez-López, R., Macías, F., Carrero, S., et al., 2019. Mineralogically-induced metal partitioning during the evaporative precipitation of efflorescent sulfate salts from acid mine drainage. Chem. Geol. 530, 119339. https://doi.org/10.1016/j.chemgeo.2019.119339.

Blowes, D.W., Ptacek, C.J., Jambor, J.L., Weisener, C.G., Paktunc, D., Gould, W.D., Johnson, D.B., 2003. The geochemistry of acid mine drainage. Environ. Geochem. 149–204, 9.

Byrne, P., Onnis, P., Runkel, R.L., Frau, I., Lynch, S.F., Edwards, P., 2020. Critical shifts in trace metal transport and remediation performance under future low river flows. Environ. Sci. Technol. 54 (24), 15742–15750. https://doi.org/10.1021/acs.est.0c04016.

Camacho, C., Negro, J.J., Elmberg, J., Fox, A.D., Nagy, S., Pain, D.J., Green, A.J., 2022. Groundwater extraction poses extreme threat to Doñana World Heritage site. Nat. Ecol. Evol. 6 (6), 654–655. https://doi.org/10.1038/s41559-022-01763-6.

Cánovas, C.R., Hubbard, C.G., Olías, M., Nieto, J.M., Black, S., Coleman, M.L., 2008. Hydrochemical variations and contaminant load in the Río Tinto (Spain) during flood events. J. Hydrol. 350 (1–2), 25–40. https://doi.org/10.1016/j.jhydrol.2007.11.022.

Cánovas, C.R., Macías, F., Olías, M., López, R.P., Nieto, J.M., 2017. Metal-fluxes characterization at a catchment scale: study of mixing processes and end-member analysis in the Meca River watershed (SW Spain). J. Hydrol. 550, 590–602. https://doi.org/10.1016/j.jhydrol.2017.05.037.

Cánovas, C.R., Macías, F., Pérez-López, R., 2016b. Metal and acidity fluxes controlled by precipitation/dissolution cycles of sulfate salts in an anthropogenic mine aquifer. J. Contam. Hydrol. 188, 29–43. https://doi.org/10.1016/j.jconhyd.2016.02.005.

Cánovas, C.R., Olías, M., Macias, F., Torres, E., San Miguel, E.G., Galván, L., et al., 2016a. Water acidification trends in a reservoir of the Iberian Pyrite Belt (SW Spain). Sci. Total Environ. 541, 400–411. https://doi.org/10.1016/j.scitotenv.2015.09.070.

Cánovas, C.R., Olías, M., Sarmiento, A.M., Nieto, J.M., Galván, L., 2012. Pollutant transport processes in the Odiel River (SW Spain) during rain events. Water Resour. Res. 48 (6). https://doi.org/10.1029/2011WR011041.

Caraballo, M.A., Macías, F., Nieto, J.M., Ayora, C., 2016. Long term fluctuations of groundwater mine pollution in a sulfide mining district with dry Mediterranean climate: implications for water resources management and remediation. Sci. Total Environ. 539, 427–435. https://doi.org/10.1016/j.scitotenv.2015.08.156.

CEDEX, 2011. Estudio preliminar sobre el proyecto del embalse de Alcolea en el río Odiel: calidad del agua y medidas para su utilización. Informe Técnico. In: Centro De Estudios Y Experimentación De Obras Públicas. Madrid, 72 pp. + 2 Anejos.

European Council, 2000. Directive 2000/60/EC of the European Parliament and of the Council of 23 October 2000 establishing a framework for Community action in the

field of water policy. Off. J. Eur. Communities - Legislation 327, 1–84. http://data.europa.eu/eli/dir/2000/60/oj.
European Council, 2020. Directive (EU) 2020/2184 of the European Parliament and of the council of 16 December 2020 on the quality of water intended for human consumption. Off. J. Eur. Communities - Legislation 435, 1–62. http://data.europa.eu/eli/dir/2020/2184/oj.
Ficklin, W.H., Plumlee, G.S., Smith, K.S., McHugh, J.B., 1992. Geochemical classification of mine drainages and natural drainages in mineralized areas. In: International Symposium on water-rock Interaction, pp. 381–384.
Galván, L., Olías, M., Cánovas, C.R., Sarmiento, A.M., Nieto, J.M., 2016. Hydrological modeling of a watershed affected by acid mine drainage (Odiel River, SW Spain). Assessment of the pollutant contributing areas. J. Hydrol. 540, 196–206. https://doi.org/10.1016/j.jhydrol.2016.06.005.
Galván, L., Olías, M., Cerón, J.C., de Villaran, R.F., 2021. Inputs and fate of contaminants in a reservoir with circumneutral water affected by acid mine drainage. Sci. Total Environ. 762, 143614. https://doi.org/10.1016/j.scitotenv.2020.143614.
Gatz, D.F., Smith, L., 1995. The standard error of a weighted mean concentration—I. Bootstrapping vs other methods. Atmos. Environ. 29 (11), 1185–1193. https://doi.org/10.1016/1352-2310(94)00210-C.
Grande, J.A., Jiménez, A., Romero, S., de la Torre, M.L., Gómez-Olivera, T., 2010. Quantification of heavy metals from AMD discharged into a public water supply dam in the Iberian Pyrite Belt (SW Spain) using centered moving average. Water, Air, Soil Pollut. 212 (1), 299–307. https://doi.org/10.1007/s11270-010-0343-y.
Helsel, D.R., Hirsch, R.M., Ryberg, K.R., Archfield, S.A., Gilroy, E.J., 2020. Statistical Methods in Water Resources. U.S. Geological Survey Techniques and Methods, p. 458. https://doi.org/10.3133/tm4a3 book 4, chap. A3.
Igarashi, T., Oyama, T., 2000. Deterioration of water quality in a reservoir receiving pyrite-bearing rock drainage and its geochemical modeling. Eng. Geol. 55 (1–2), 45–55. https://doi.org/10.1016/S0013-7952(99)00105-2.
Jacobs, J., Testa, S.M., Alpers, C.N., Nordstrom, D.K., 2016. An overview of environmental impacts and mine reclamation efforts at Iron Mountain, Shasta County, California. In: Anderson, R., Ferriz, H. (Eds.), Applied Geology in California, Association of Environmental & Engineering Geologists. Star Publishing Company, Belmont, CA, pp. 427–446. https://pubs.usgs.gov/publication/70178907.
Jamieson, H.E., Robinson, C., Alpers, C.N., McCleskey, R.B., Nordstrom, D.K., Peterson, R.C., 2005. Major and trace element composition of copiapite-group minerals and coexisting water from the Richmond mine, Iron Mountain, California. Chem. Geol. 215 (1–4), 387–405. https://doi.org/10.1016/j.chemgeo.2004.10.001.
Jurado-Almonte, J.M., Díaz-Diego, J., 2022. The role of the Andalusian Institute for Agrarian Reform (IARA) in irrigation expansion: the case of the Chanza irrigation project (Huelva, Spain). Water 14 (18), 2931. https://doi.org/10.3390/w14182931.
Keith, D.C., Runnells, D.D., Esposito, K.J., Chermak, J.A., Levy, D.B., Hannula, S.R., et al., 2001. Geochemical models of the impact of acidic groundwater and evaporative sulfate salts on Boulder Creek at Iron Mountain, California. Appl. Geochem. 16 (7–8), 947–961. https://doi.org/10.1016/S0883-2927(00)00080-9.
Kimball, B.A., Bianchi, F., Walton-Day, K., Runkel, R.L., Nannucci, M., Salvadori, A., 2007. Quantification of changes in metal loading from storm runoff, Merse River (Tuscany, Italy). Mine Water Environ. 26 (4), 209–216. https://doi.org/10.1007/s10230-007-0020-6.
Kirby, C.S., Cravotta III, C.A., 2005. Net alkalinity and net acidity 1: theoretical considerations. Appl. Geochem. 20 (10), 1920–1940. https://doi.org/10.1016/j.apgeochem.2005.07.002.
León, R., Macías, F., Cánovas, C.R., Pérez-López, R., Ayora, C., Nieto, J.M., Olías, M., 2021. Mine waters as a secondary source of rare earth elements worldwide: the case of the Iberian Pyrite Belt. J. Geochem. Explor. 224, 106742. https://doi.org/10.1016/j.gexplo.2021.106742.
León, R., Millán-Becerro, R., Macías, F., Cánovas, C.R., Neculita, C.M., Ayora, C., Nieto, J.M., 2025. Dispersed alkaline substrate passive treatment technology for highly contaminated acid mine drainage: 20 years of successful application. Water Res., 124683 https://doi.org/10.1016/j.watres.2025.124683.
Lottermoser, B.G., 2010. Mine water. In: Mine Wastes: Characterization, Treatment and Environmental Impacts. Springer Berlin Heidelberg, Berlin, Heidelberg, pp. 119–203. https://doi.org/10.1007/978-3-642-12419-8.
Macías, F., Pérez-López, R., Caraballo, M.A., Canovas, C.R., Nieto, J.M., 2017. Management strategies and valorization for waste sludge from active treatment of extremely metal-polluted acid mine drainage: a contribution for sustainable mining. J. Clean. Prod. 141, 1057–1066. https://doi.org/10.1016/j.jclepro.2016.09.181.
Manning, A.H., Petach, T.N., Runkel, R.L., McKnight, D.M., 2024. Climate-driven increases in stream metal concentrations in mineralized watersheds throughout the Colorado Rocky Mountains, USA. Water Resour. Res. 60 (4). https://doi.org/10.1029/2023WR036062 e2023WR036062.
Moreno-González, R., Macías, F., Olias, M., Canovas, C.R., 2022. Temporal evolution of acid mine drainage (AMD) leachates from the abandoned tharsis mine (Iberian Pyrite Belt, Spain). Environ. Pollut. 295, 118697. https://doi.org/10.1016/j.envpol.2021.118697.
Munk, L., Faure, G., 2004. Effects of pH fluctuations on potentially toxic metals in the water and sediment of the Dillon Reservoir, Summit County, Colorado. Appl. Geochem. 19 (7), 1065–1074. https://doi.org/10.1016/j.apgeochem.2004.01.006.
Musolff, A., Schmidt, C., Selle, B., Fleckenstein, J.H., 2015. Catchment controls on solute export. Adv. Water Resour. 86, 133–146. https://doi.org/10.1016/j.advwatres.2015.09.026.
Newman, C.P., Navarre-Sitchler, A., Runkel, R.L., Cowie, R., 2025. Concentration-discharge relations and transient metal loads reveal spatiotemporal variability in solute-generation mechanisms in a mine-affected watershed. J. Contam. Hydrol. 269, 104513. https://doi.org/10.1016/j.jconhyd.2025.104513.
Nieto, J.M., Sarmiento, A.M., Canovas, C.R., Olías, M., Ayora, C., 2013. Acid mine drainage in the Iberian Pyrite Belt: 1. Hydrochemical characteristics and pollutant load of the Tinto and Odiel rivers. Environ. Sci. Pollut. Control Ser. 20 (11), 7509–7519. https://doi.org/10.1007/s11356-013-1634-9.
Nordstrom, D.K., 2009. Acid rock drainage and climate change. J. Geochem. Explor. 100 (2–3), 97–104. https://doi.org/10.1016/j.gexplo.2008.08.002.
Nordstrom, D.K., 2011. Hydrogeochemical processes governing the origin, transport and fate of major and trace elements from mine wastes and mineralized rock to surface waters. Appl. Geochem. 26 (11), 1777–1791. https://doi.org/10.1016/j.apgeochem.2011.06.002.
Nordstrom, D.K., Alpers, C.N., Coston, J.A., Taylor, H.E., McCleskey, R.B., Ball, J.W., et al., 1999. Geochemistry, toxicity, and sorption properties. In: US Geological Survey Toxic Substances Hydrology Program: Proceedings of the Technical Meeting, Charleston, South Carolina, March 8-12, 1999, vol. 1. US Department of the Interior, US Geological Survey, p. 289, 99.
Olías, M., Cánovas, C.R., Basallote, M.D., Macías, F., Nieto, J.M., Pérez-López, R., Sarmiento, A.M., 2024. The problem of acid mine drainage in the Iberian Pyrite Belt (IPB): diagnosis and treatment measures, vol. 1. Servicio de Publicaciones de la Universidad de Huelva, p. 200. https://www.uhu.es/publicaciones/?q=libros&code=1347.
Olías, M., Cánovas, C.R., Basallote, M.D., Macías, F., Pérez-López, R., González, R.M., et al., 2019. Causes and impacts of a mine water spill from an acidic pit lake (Iberian Pyrite Belt). Environ. Pollut. 250, 127–136. https://doi.org/10.1016/j.envpol.2019.04.011.
Olías, M., Cánovas, C.R., Nieto, J.M., Sarmiento, A.M., 2006. Evaluation of the dissolved contaminant load transported by the Tinto and Odiel rivers (South West Spain). Appl. Geochem. 21 (10), 1733–1749. https://doi.org/10.1016/j.apgeochem.2006.05.009.
Olías, M., Nieto, J.M., Sarmiento, A.M., Cánovas, C.R., Galván, L., 2011. Water quality in the future Alcolea Reservoir (Odiel River, SW Spain): a clear example of the inappropriate management of water resources in Spain. Water Resour. Manag. 25, 201–215. https://doi.org/10.1007/s11269-010-9695-8.
Palma, P., Ledo, L., Alvarenga, P., 2015. Assessment of trace element pollution and its environmental risk to freshwater sediments influenced by anthropogenic contributions: the case study of Alqueva reservoir (Guadiana Basin). Catena 128, 174–184. https://doi.org/10.1016/j.catena.2015.02.002.
Parkhurst, D.L., Appelo, C.A.J., 2013. Description of input and examples for PHREEQC version 3—a computer program for speciation, batch-reaction, one-dimensional transport, and inverse geochemical calculations. US Geol. Surv. Techn. Method 6 (A43), 497. https://doi.org/10.3133/tm6A43.
Pérez-López, R., Cánovas, C.R., Macías, F., Basallote, M.D., Freydier, R., Olías, M., Nieto, J.M., 2025. Tracing acid mine drainage from an accidental spill on the Estuary of Huelva (SW Spain). Environ. Pollut. 372, 126033. https://doi.org/10.1016/j.envpol.2025.126033.
Petach, T.N., Runkel, R.L., Cowie, R.M., McKnight, D.M., 2021. Effects of hydrologic variability and remedial actions on first flush and metal loading from streams draining the Silverton caldera, 1992–2014. Hydrol. Process. 35 (11), e14412. https://doi.org/10.1002/hyp.14412.
Rakotonimaro, T.V., Neculita, C.M., Bussière, B., Benzaazoua, M., Zagury, G.J., 2017. Recovery and reuse of sludge from active and passive treatment of mine drainage-impacted waters: a review. Environ. Sci. Pollut. Control Ser. 24 (1), 73–91. https://doi.org/10.1007/s11356-016-7733-7.
Reisman, D.J., Sundaram, V., Al-Abed, S.R., Allen, D., 2007. Statistical validation of sulfate quantification methods used for analysis of acid mine drainage. Talanta 71 (1), 303–311. https://doi.org/10.1016/j.talanta.2006.04.002.
Romero-Matos, J., Sánchez-López, L., León, R., Runkel, R.L., Nordstrom, D.K., Cánovas, C.R., et al., 2026. Characterization and modeling approach for planning restoration strategies in a complex basin affected by acid mine drainage. J. Environ. Manag. 397, 127486. https://doi.org/10.1016/j.jenvman.2025.127486.
Runkel, R.L., Kimball, B.A., Nimick, D.A., Walton-Day, K., 2016. Effects of flow regime on metal concentrations and the attainment of water quality standards in a remediated stream reach, Butte, Montana. Environ. Sci. Technol. 50 (23), 12641–12649. https://doi.org/10.1021/acs.est.6b03190.
Sáinz, A., Grande, J.A., De la Torre, M.L., Sánchez-Rodas, D., 2002. Characterisation of sequential leachate discharges of mining waste rock dumps in the Tinto and Odiel rivers. J. Environ. Manag. 64 (4), 345–353. https://doi.org/10.1006/jema.2001.0497.
Sánchez-España, J., Pamo, E.L., Santofimia, E., Aduvire, O., Reyes, J., Barettino, D., 2005. Acid mine drainage in the Iberian Pyrite Belt (Odiel river watershed, Huelva, SW Spain): geochemistry, mineralogy and environmental implications. Appl. Geochem. 20 (7), 1320–1356. https://doi.org/10.1016/j.apgeochem.2005.01.011.
Sánchez-España, J., Yusta, I., Diez-Ercilla, M., 2011. Schwertmannite and hydrobasaluminite: a re-evaluation of their solubility and control on the iron and aluminium concentration in acidic pit lakes. Appl. Geochem. 26 (9–10), 1752–1774. https://doi.org/10.1016/j.apgeochem.2011.06.020.
Sarmiento, A.M., Nieto, J.M., Olías, M., Cánovas, C.R., 2009. Hydrochemical characteristics and seasonal influence on the pollution by acid mine drainage in the Odiel river Basin (SW Spain). Appl. Geochem. 24 (4), 697–714. https://doi.org/10.1016/j.apgeochem.2008.12.025.
Singh, A.K., Singh, A., Engelhardt, M., 1999. Some Practical Aspects of Sample Size and Power Computations for Estimating the Mean of Positively Skewed Distributions in Environmental Applications. U.S. Environmental Protection Agency, p. 37.
Van Vliet, M.T., Thorslund, J., Strokal, M., Hofstra, N., Flörke, M., Ehalt Macedo, H., et al., 2023. Global river water quality under climate change and hydroclimatic extremes. Nat. Rev. Earth Environ. 4 (10), 687–702. https://doi.org/10.1038/s43017-023-00472-3.

World Health Organization, 2022. Guidelines for drinking-water Quality: Fourth Edition Incorporating the First and Second Addenda. World Health Organization (WHO), Geneva. ISBN 978-92-4-004506-4. https://www.who.int/publications/i/item/9789240045064.

Younger, P., 1997. The longevity of minewater pollution: a basis for decision making, p 457-466. Sci. Total Environ. https://doi.org/10.1016/S0048-9697(96)05383-1, 194&195.

Younger, P.L., 2000. Predicting temporal changes in total iron concentrations in groundwaters flowing from abandoned deep mines: a first approximation. J. Contam. Hydrol. 44 (1), 47–69. https://doi.org/10.1016/S0169-7722(00)00090-5.

Zhang, C., Wu, P., Tang, C., Tao, X., Han, Z., Sun, J., Liu, H., 2013. The study of soil acidification of paddy field influenced by acid mine drainage. Environ. Earth Sci. 70 (7), 2931–2940. https://doi.org/10.1007/s12665-013-2351-x.